



# Analysis of the risk-targeting approach to defining ground motion for seismic design: a case study of Iran

Amir Reza Taherian<sup>1</sup> · Afshin Kalantari<sup>1</sup>

Received: 18 August 2020 / Accepted: 10 December 2020 / Published online: 5 January 2021  
© The Author(s), under exclusive licence to Springer Nature B.V. part of Springer Nature 2021

## Abstract

Modern seismic codes employed the uniform hazard basis for seismic design, which defines design ground motion with a fixed return period for different sites. Seismic design for uniform hazard ground motion does not lead to the goal of uniform structural safety. As a potential solution to address this problem, the risk-targeting approach has been considered in recent years. This study aims to investigate the changes applied by this approach to the current uniform hazard ground motions. For this purpose, hazard curves for Iran from the Earthquake Model of Middle East (EMME14) have been used. The risk-targeting approach has been performed in two cases, once considering GMs with a 475 year return period and then considering GMs with a 2475 year return period. For each case, a generic fragility function for buildings has been defined. A 1% probability of collapse in 50 years was selected as the target risk in both cases. For each case, the map of the distribution of the theoretical collapse risk is presented. It was discussed that by employing a generic fragility function, the risk-targeting could not guarantee to harmonize risk amongst the sites with different hazard levels, but it could have such an impact for the sites with the same design GM but the different slope of hazard curves. Finally, it was found that basing the seismic design on the 2% in 50 years GMs level leads to a more uniform collapse risk across the country.

**Keywords** Building collapse assessment · Risk-targeted design basis · Seismic hazard · Structural reliability

## 1 Introduction

The basics of probabilistic seismic hazard analysis were presented by Cornell (1968). This method has been the basis of seismic loading in seismic codes for more than 40 years. The principal output of this method is Uniform Hazard Ground Motion

---

✉ Afshin Kalantari  
A.kalantari@iiees.ac.ir

Amir Reza Taherian  
amirtaherian1994@gmail.com

<sup>1</sup> Structural Engineering Research Center, International Institute of Earthquake Engineering and Seismology, Tehran, Iran

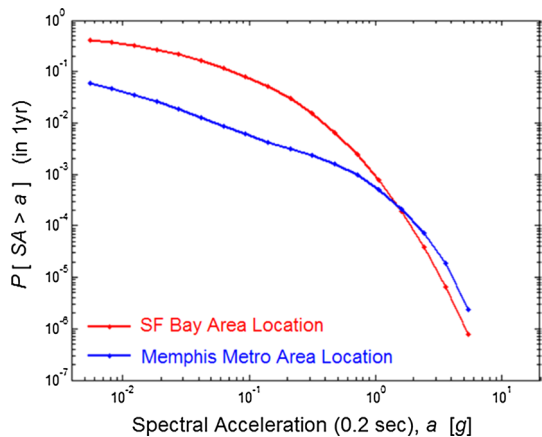
(UHGM) maps. These maps provide the design ground motion values for earthquakes with the same return period for different regions.

Prior to the 2000s, design ground motion values for the 475-year return period earthquake, which has a 10% in 50 years Exceedance Probability (EP), were presented in US seismic codes. The next generation of US seismic codes (the 1997 uniform building code, NEHRP 2000, ASCE7-05) have presented the Maximum Considered Earthquake (MCE) ground motion maps, which contain values with 2% in 50 years EP. However, this change in the US seismic codes was met with much criticism and debate. The main point of discussion was the new state of design in California and Memphis. The change made the design base the same in the two areas of Memphis, located in the New Madrid Seismic Zone (NMSZ) and California. Stein et al. (2003) stated that according to FEMA's estimates, buildings in Memphis are 5 to 10 times less likely to be damaged than San Francisco or Los Angeles; therefore, the design basis in these two areas should not be the same. Moreover, large earthquakes are less frequent in New Madrid than in southern California. Hence, Stein et al. (2003) argued that the new code should not be adopted unless justified by careful analysis.

Frankel (2003), In defense of the new state of design in Memphis, stated that even though magnitude-7 earthquakes may be less frequent in the NMSZ than in California, they can produce similar probabilities of damaging ground motions since New Madrid earthquakes will generate higher ground motions than California earthquakes with the same magnitude.

The Memphis-California situation is an applicable and clear example of challenging the uniform hazard philosophy. As discussed by Luco et al. (2007), the seismic design of buildings for UHGM does not lead to an equal risk of collapse in different regions. For instance, Luco et al. (2007) showed that the probability of collapse of buildings in San Francisco is up to 30% higher than in Memphis. There are two main reasons for this: The first reason is that this method only takes one point of hazard curve into account, regardless of the differences in the shape of hazard curves. Figure 1 shows examples of hazard curves for San Francisco and Memphis with almost the same MCE but very different shapes. Besides that, there are uncertainties in the collapse capacity of structures. The combination of these two reasons has led to an unequal probability of collapse in different areas.

**Fig. 1** Examples of hazard curves for  $S_a$  (0.2 s) for two sites located in San Francisco and Memphis (Luco et al. 2007)



To solve this problem, as an alternative to the uniform hazard approach, Luco et al. (2007) proposed a method called the risk-targeting method for calculating design GM. Employing this method, GM values for the design of buildings for a target collapse probability is achieved. Based on the study of Luco et al. (2007), Risk-Targeted Maximum Considered Earthquake ( $MCE_R$ ) ground motion maps were presented in the 2009 update of NEHRP provisions and ASCE7-10 (2010). By decreasing MCE values in the center and eastern parts of the US, the risk-targeting approach established a balance in the distribution of the collapse probability across the country. As a result, the MCE ground motion values in Memphis decreased by up to 30%.

Hereafter, studies were conducted to present the risk-targeted design maps in different regions. The most remarkable studies in this field were made by Douglas et al. (2013) for France and Silva et al. (2016) for Europe. Also, Taherian and Kalantari (2019) have developed risk-targeted design maps for Iran. However, the risk-targeting approach has not yet been included in the seismic codes of these regions.

The main question of this research is, how does the risk-targeting approach change the UHGM in areas of different hazard levels? To answer this question, using mean PGA hazard curves from the Earthquake Model of Middle-East (EMME14), risk-targeted design GM is calculated for Iran in two cases: once considering 10% EP in 50 years GM, and then considering 2% EP in 50 years GM as the UHGM. In each case, the results were analyzed to better understand the effectiveness of the proposed method.

## 2 An overview of the risk-targeting approach

By combining a site-specific hazard curve and a building collapse fragility curve, the mean annual frequency of collapse is calculated using Eq. (1), an application of the total probability theorem.

$$\lambda_C = \int_0^{\infty} P(C|im) \cdot |d\lambda_{IM}(im)| \tag{1}$$

where  $\lambda_C$  is the mean annual frequency of collapse,  $\lambda_{IM}$  is the mean annual frequency of exceedance of ground motion intensity measure. Under the Poisson distribution assumption, the probability of collapse in  $t$  years is computed by Eq. (2).

$$P_c \text{ in } t \text{ years} = 1 - (1 - \lambda_C)^t \tag{2}$$

Generally, in risk-targeting, a generic collapse fragility function is assumed for buildings designed with the referenced code. The fragility function is usually defined using the log-normal distribution. The log-normal distribution is defined using a median (50th percentile) and a logarithmic standard deviation  $\beta$ . However, this function can be parametrized by  $\beta$  and any other percentiles of the probability distribution (Luco et al. 2007). There is a direct relationship between the median collapse capacity of a structure and its design GM. Assuming a probability of collapse at design GM of  $X$  and uncertainty in collapse capacity  $\beta$ , the generic-fragility function is defined using Eq. (3).

$$P(C|im) = \Phi \left[ \frac{\ln im - (\ln c_X - \Phi^{-1}(X), \beta)}{\beta} \right] \tag{3}$$

where the  $P(\text{Clim})$  is the probability of collapse of the building under a specific intensity measure,  $\Phi[\cdot]$  is the standard normal cumulative distribution function (CDF),  $C_X$  is  $X$  percentile collapse capacity of the structure. The parameter  $C_X$  is equal to the design GM of the buildings. To define the generic fragility function, we should have a reasonable estimation of  $X$  and  $\beta$ .

In the study of Luco et al. (2007), these parameters were selected based on the collapse assessment of different building systems in the ATC-63 project (FEMA 2009). In contrast, due to the lack of sufficient studies on developing analytical fragility curves, other studies have used sensitivity analyses to determine the generic fragility parameters. The information on the spectral ordinates, reference hazard level, and generic fragility function parameters used in different studies are shown in Table 1.

According to Table 1, an essential difference between Luco et al. (2007) and other studies is the reference hazard level. In Europe and Iran, buildings are currently designed for GMs with 10% EP in 50 years. The effect of the reference hazard level on the results will be discussed in the following sections.

Defining the collapse fragility curve as a function of the design GM allows us to achieve a target collapse probability by changing the design GM values. That is a logical assumption; the higher the design GM, the higher the collapse capacity, and therefore the lower the probability of collapse. According to the risk-targeting algorithm presented by Luco et al. (2007), the value of  $C_X$  changes iteratively until the target collapse probability is achieved for each site. From the division of risk-targeted GM to UHGM, the risk coefficient ( $C_R$ ) is achieved. The distribution of  $C_R$  values shows how UHGM changes in different sites.

Since imposing significant adjustments in the current UHGMs is not desired, a value close to the average collapse probability in the region is selected as the target collapse risk. Therefore, a reasonable estimation of the current distribution of collapse risk of buildings in the region under study is required. By placing the UHGM as  $C_X$  in Eq. (3), the spatial distribution of theoretical collapse risk is obtained. This map shows in which sites the UHGM should be increased and where it should be decreased.

### 3 Distribution of seismic hazard in Iran

In this study, PGA hazard curves from the Earthquake Model of Middle-East (EMME14) have been employed. The EMME14 project was carried out between 2010 and 2014 to provide a harmonized seismic hazard assessment without country border limitations. The result covers eleven countries: Afghanistan, Armenia, Azerbaijan, Cyprus, Georgia, Iran, Jordan, Lebanon, Pakistan, Syria, and Turkey, which span one of the seismically most active regions on Earth in response complex interactions between four major tectonic plates, i.e., Africa, Arabia, India, and Eurasia. (Danciu et al. 2017).

**Table 1** Elements of the risk-targeting approach employed in different studies

	Spectral ordinates	Reference hazard level	$X$	$\beta$
Luco et al. (2007)	Sa (0.2 s), Sa(1 s)	2% in 50 years	$10^{-1}$	0.8
Douglas et al. (2013)	PGA	10% in 50 years	$10^{-5}$	0.5
Silva et al. (2016)	PGA	10% in 50 years	$10^{-3}$	0.6
Taherian and Kalantari (2019)	PGA	10% in 50 years	$10^{-2}$	0.8

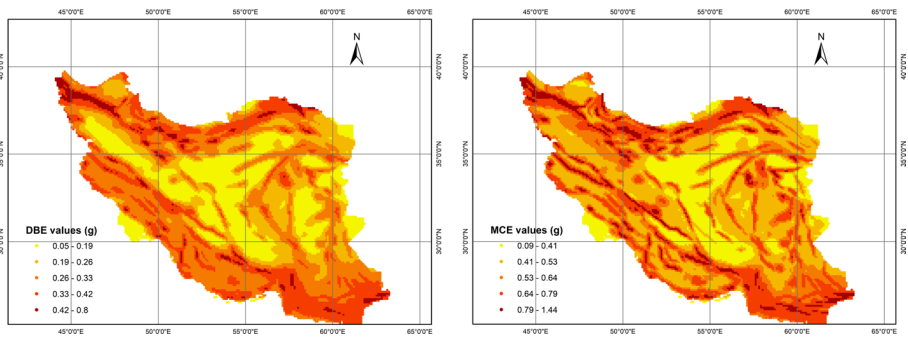


**Fig. 2** Spatial distribution of Seismic hazard in terms of **a** PGA with 10% in 50 years EP (DBE), **b** PGA with 2% in 50 years EP (MCE), in Iran

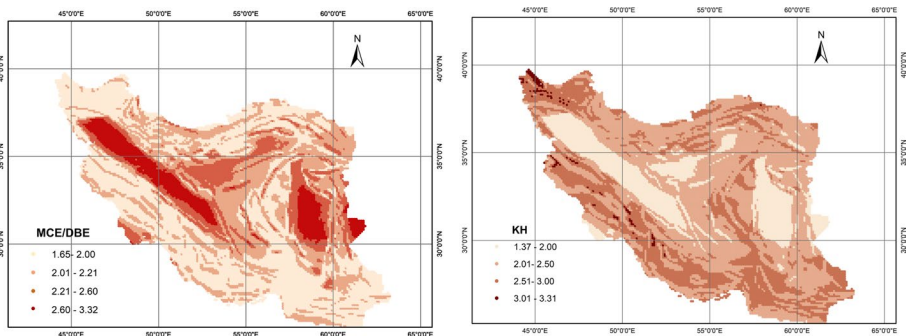


**Fig. 3** Spatial distribution of **a** MDR values, **b**  $K_H$  values in the country

In this study, the PGA values with a 10% EP in 50 years are called Design Basis Earthquake, DBE, and the PGA values with a 2% EP in 50 years are called Maximum Considered Earthquake, MCE. Figure 2 shows the spatial distribution of seismic hazard in terms of DBE and MCE values in the country.

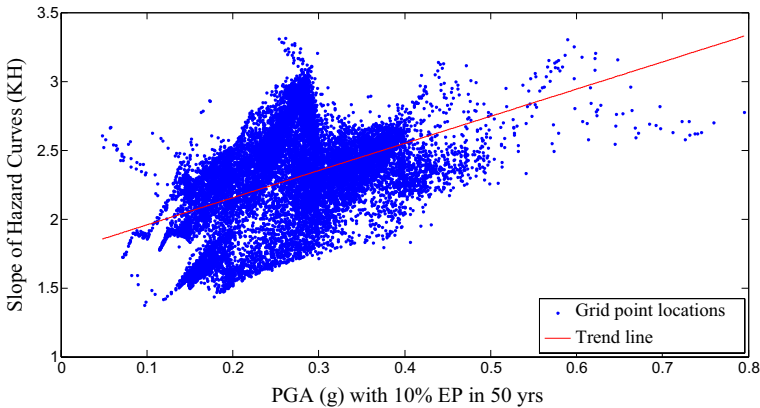
As discussed earlier, the collapse capacity of structures is uncertain. Therefore, the shape of the hazard curve (or its local slope) is essential in the collapse risk of structures. The slope of the hazard curve ( $K_H$ ) is the rate at which ground motion amplitudes increase as probability decreases (Atkinson 2004). Different formulations of the parameter  $K_H$  presented and discussed by Gkimprxis et al. (2019). In this article,  $K_H$  is defined as the logarithmic slope of the hazard curve between MCE and DBE, using Eq. (4) (Jalayer and Cornell 2003).

$$K_H = \frac{\log\left(\frac{H(DBE)}{H(MCE)}\right)}{\log\left(\frac{MCE}{DBE}\right)} = \frac{\log\left(\frac{2.1 \times 10^{-3}}{4.04 \times 10^{-4}}\right)}{\log\left(\frac{MCE}{DBE}\right)} \tag{4}$$

where  $H(\cdot)$  is the annual probability of exceedance of a specific level of hazard. According to Eq. (4), the parameter  $K_H$  is inversely related to the MCE to DBE Ratio (MDR). Figure 3 shows the distribution of the  $K_H$  and MDR values in the country. A simple statistical

**Table 2** Statistical analysis of the seismic hazard in the country

	5th percentile	95th percentile	Mean	STD
DBE (g)	0.15	0.40	0.27	0.08
MCE (g)	0.33	0.81	0.55	0.15
KH	1.63	2.85	2.29	0.35
MCE to DBE Ratio (MDR)	1.78	2.75	2.11	0.28

**Fig. 4** Distribution of the slope of hazard curves in different seismic hazard levels of the country

analysis of seismic hazard in the country is shown in Table 2. usually, in Iranian engineering practices, a factor of 1.5 is employed to shift from DBE to MCE level. Nonetheless, according to Table 2, the MDR values could vary significantly with location. According to EMME14 results, the mean of MDR values in the country is 2.11, with a dispersion of 0.28.

From Fig. 3, it can be observed that in areas from northwest to central parts of the country, which is called the Sanandaj-Sirjan Zone (SSZ), as well as Central-Eastern Iran (the Lut block), the  $K_H$  values are very low, or in other words, MDR values are very high (up to 3). In general, in low-to moderate-hazard areas where severe earthquakes happen rarely, the slopes of the hazard curves are lower. Figure 4 shows the distribution of  $K_H$  values in different seismic hazard levels of the country. As stated by Atkinson (2004), in the active regions, ground motion amplitudes may grow relatively slowly as the probability is lowered from 1/100 to 1/1000; this is because the 1/100 motion may already represent nearby earthquakes close to the maximum magnitude. In inactive regions, 1/100 motions are small but grow steadily as the probability level is lowered.

It should be noted that during the development of the EMME14 source model, the SSZ and Lut block have been modeled as the stable continental region (SCR). The GMPEs presented by Toro et al. (1997), Campell (2003), Atkinson and Bore (2006) for the Central and Eastern US (CEUS) have been selected for the SCRs in the Middle East region. Frankel (2004) explained that earthquakes in the CEUS and elsewhere in eastern North America produce higher ground motions at high frequencies (for PGA and S.A. at about 2 Hz and above) for a given distance than western US earthquakes with the same magnitudes. This fact could justify high PGA values at low probability levels in central Iran's hazard curves.

However, the EMME14 results are inconsistent with the seismicity of the SSZ. This area has relatively low seismic activity. Besides, no significant earthquake has been recorded in this area so far (Safaei 2009; Nadimi 2012). Nonetheless, the occurrence of historical earthquakes indicates that this zone is active. For instance, the Isfahan earthquake of 1344 killed about 20 people and destroyed the city wall and some houses (Ambraseys and Melville 1982; Safaei 2009). Therefore, site-specific studies are required to validate EMME14 results for central Iran.

### 4 Discussion and results

In this section, the results of the risk-targeting approach are presented in two cases. In the first case, risk-targeted calculations are performed based on DBE values at each point of the country. Similarly, in the second case, calculations are performed based on the MCE level. In the end, the results for each case are compared. For each case, a generic fragility function should be defined.

In this study, a series of sensitivity analyses have been performed to select the generic fragility function parameters for each case. A 1% probability of collapse in 50 years is selected as the target collapse risk in both cases. Given the target collapse risk, the generic fragility function parameters have been selected to make the least changes in the UHGM defined in each case. In the following, assuming the different values of  $X$  ranging from  $10^{-1}$  to  $10^{-5}$  and  $\beta$  ranging from 0.5 to 0.8, the annual collapse rates were calculated for all over the country. Figure 5 indicates the relation between the annual probability of collapse and different combinations of  $X$  and  $\beta$ . The maximum and minimum amounts of collapse risk for each case are shown in Fig. 5.

Another important point in choosing the parameters  $X$  and  $\beta$  is that the median of the fragility curves should be within a reasonable range. For different values of  $X$  and  $\beta$ , the range of median of fragility curves can be observed in Table 3. As shown in Table 3, selecting some values of  $X$  and  $\beta$  leads to an unrealistically high estimation of the median of fragility curves and should be avoided.

According to Fig. 5, assuming the parameters  $X=10^{-2}$  and  $\beta=0.80$  for the first case and assuming  $X=10^{-1}$  and  $\beta=0.80$  for the second case would result in modest changes in

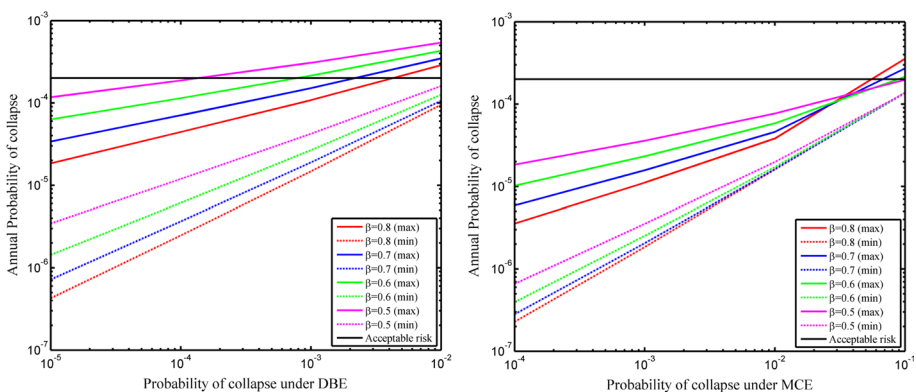


**Fig. 5** Relation of the annual probability of collapse with the parameters  $X$  and  $\beta$  based on a the DBE level b the MCE level defined by the EMME14

**Table 3** Results of the median of generic fragility curves based on the DBE and MCE level defined by the EMME14 and assuming different values of  $X$  and  $\beta$ 

X		$\beta=0.5$		$\beta=0.6$		$\beta=0.7$		$\beta=0.8$	
		Median (g)		Median (g)		Median (g)		Median (g)	
		DBE	MCE	DBE	MCE	DBE	MCE	DBE	MCE
$10^{-5}$	Max	6.71	12.15	10.27	18.62	15.73	28.52	24.10	43.69
	Min	0.41	0.76	0.62	1.17	0.95	1.79	1.46	2.74
$10^{-4}$	Max	5.09	9.25	7.38	13.42	10.70	19.46	15.51	28.22
	Min	0.31	0.58	0.45	0.84	0.65	1.22	0.94	1.77
$10^{-3}$	Max	3.72	6.75	5.06	9.20	6.89	12.53	9.38	17.07
	Min	0.22	0.42	0.31	0.58	0.42	0.79	0.57	1.07
$10^{-2}$	Max	2.54	4.61	3.21	5.82	4.05	7.34	5.11	9.26
	Min	0.15	0.29	0.19	0.37	0.24	0.46	0.31	0.58
$10^{-1}$	Max	1.51	2.73	1.72	3.11	1.95	3.53	2.22	4.01
	Min	0.09	0.17	0.10	0.19	0.12	0.22	0.13	0.25

UHGMs. Also, based on our judgment on the fragility of Iranian buildings, assuming these values, the median of fragility curves would be in a reasonable range.

#### 4.1 Risk-targeting based on DBE

In this case, by defining the generic fragility curves as a function of DBE values, the distribution of the theoretical probability of collapse in the country is achieved. Figure 6 shows the spatial distribution of the theoretical collapse risk in the first case. Theoretical risk means that if the probability of buildings collapsing in the event of DBE is 1% and  $\beta$  is 0.8, then the distribution of collapse risk will be following Fig. 6. In this case, the Coefficient of Variation (CoV) of the theoretical probability of collapse in the country is 22%.

Comparing Fig. 6 and Fig. 2a, one can find an opposing trend between the theoretical risk map and seismic hazard in the country, which is an unrealistic scenario. This trend is in contrast with the major conclusion of the RINTC project in Italy (Iervolino et al. 2018). This study shows that the seismic risk of buildings is directly related to the seismic hazard of the site. As stated by Cito and Iervolino (2020), one of the explanations for these results is the requirements that the code imposes regardless of the design seismic actions, that are expected to have a larger effect on the seismic safety of structures designed for low hazard sites. Moreover, as it is discussed by Cito and Iervolino (2020), the GM beyond that considered for design (which has a higher occurrence probability in high hazard sites) can also play a role with respect to this issue.

Therefore, to achieve more uniform structural safety, it is needed to increase the UHGMs in high hazard regions or decrease them in low hazard regions. However, this is not the case for the risk-targeting based on DBE. As shown in Fig. 7b, in this case, the calculated  $C_R$  values decrease as the seismic hazard of the site increase. The same trends can be observed in previous studies (Douglas et al. 2013; Silva et al. 2016; Taherian and Kalantari 2019).

The reasons for this opposing trend are explained in the two following sections.



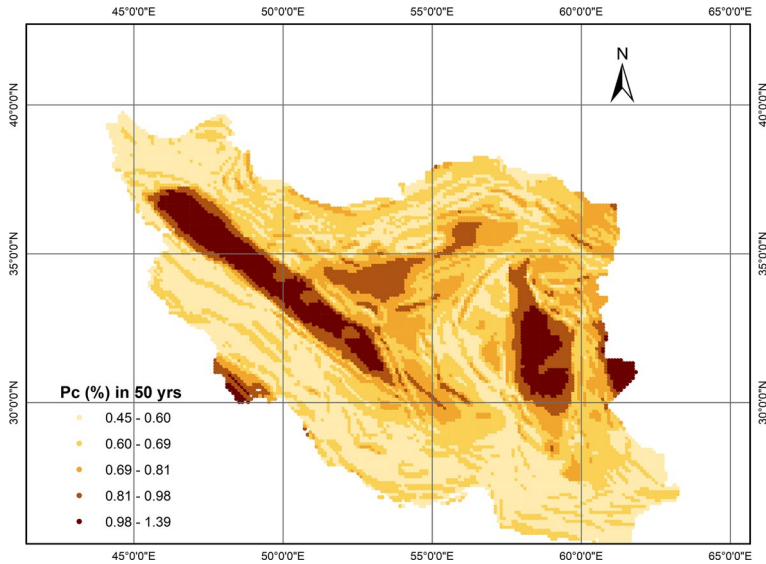


**Fig. 6** Spatial distribution of the theoretical risk of collapse in Iran considering 1% collapse probability given DBE shaking and  $\beta=0.8$

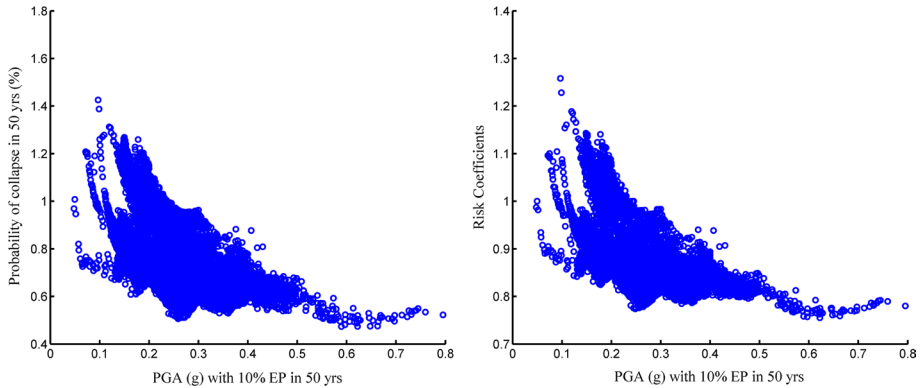


**Fig. 7** Relation of seismic hazard in terms of DBE and **a** theoretical collapse risk, **b** risk coefficients

#### 4.1.1 Assuming a fixed probability of collapse at the design GM (X)

As stated earlier, in risk-targeting, a generic fragility function is usually defined using the parameters  $\beta$  and X. Previous studies have shown that the results are sensitive to these parameters (Douglas et al. 2013; Gkimprxis et al. 2019). However, the results are more sensitive to the value of X.

Martins et al. (2018) have investigated the influence of design PGA on parameter X for RC moment-resisting frame buildings designed according to EC8. It was found that for design PGA ranging from 0.05 g to 0.40 g, parameter X varies between  $10^{-5}$  and

**Table 4** Effect of the parameter X on the median collapse capacity (g) and the theoretical collapse risk

X	$\Phi^{-1}(X)$	Median collapse capacity (g)		Probability of collapse in 50 years (%)	
		DBE=0.10 g	DBE=0.60 g	DBE=0.10 g	DBE=0.60 g
$10^{-1}$	-1.28	0.27	1.64	5.05	3.77
$10^{-2}$	-2.33	0.62	3.79	1.42	0.47
$10^{-3}$	-3.09	1.14	6.99	0.54	0.07
$10^{-4}$	-3.72	1.88	11.56	0.22	0.01
$10^{-5}$	-4.26	2.91	17.89	0.09	0.002

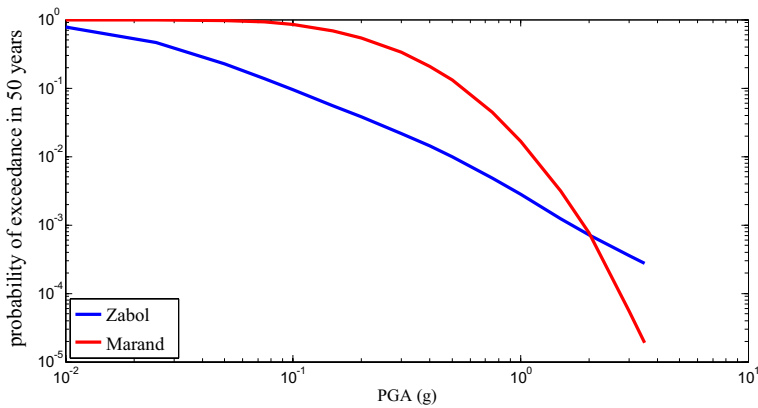


**Fig. 8** PGA hazard curves for Zabol (the maximum  $P_c$ ) and Marand (the minimum  $P_c$ )

$10^{-2}$ . Similar results were observed from the studies of Ulrich et al. (2014) and Gkim-prixis et al. (2018).

Nonetheless, in risk-targeting, X is assumed to be equal for areas of different seismicity. This assumption can explain why the collapse probabilities are higher in low hazard areas. The highest probability of collapse is 1.42%, which is calculated for Zabol with a DBE of 0.10 g. The lowest collapse probability (0.47%) is calculated for Marand with a DBE of 0.60 g. Table 4 shows the effect of selecting different values of X on the theoretical collapse risk for these sites. The parameter  $\beta$  is assumed to be 0.8 in all cases. Assuming the parameter X equal to  $10^{-2}$  for the buildings in low hazard areas has led to an underestimated collapse capacity and correspondingly overestimated calculation of the risk of collapse.

Figure 8 shows the PGA hazard curves used to generate the results of Table 4. According to Fig. 8, the hazard curve in Marand is much steeper than that of Zabol. The value of  $K_H$  in Zabol and Marand are 1.5 and 3.3, respectively. The effect of the slope of hazard curves on the results will be discussed in the following section.

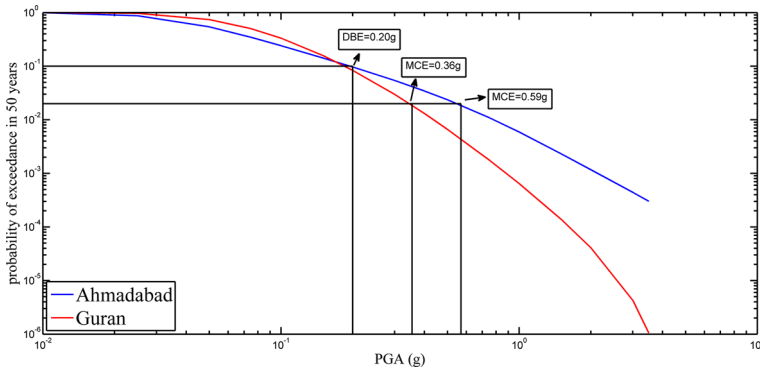


Fig. 9 Examples of PGA hazard curves for Ahmadabad and Guran

Table 5 Comparison of the results of the theoretical collapse risk for Ahmadabad and Guran

	DBE (g)	MCE (g)	MCE/DBE	$K_H$	Probability of collapse in 50 years (%)
Ahmadabad	0.20	0.59	2.90	1.5	1.13
Guran	0.20	0.36	1.80	2.57	0.65

#### 4.1.2 Low slope of hazard curves ( $K_H$ ) in low-to moderate-hazard regions

The results shown in Fig. 7 show some locations with the same DBE but a very different probability of collapse. This difference is due to the effects of the slopes of hazard curves ( $K_H$ ).

The low  $K_H$  values in the SSZ have been discussed in Sect. 3 of this paper. From Fig. 6, it can be observed that the theoretical probability of collapse in the SSZ is very higher than in most of the country. Figure 9 shows an example of PGA hazard curves for two areas with moderate seismic hazard in terms of DBE, one of which (Ahmadabad) is located in SSZ and another (Guran) located in Hormozgan province (in the southernmost point of the country). These are locations with the same DBE equal to 0.20 g, but with very different slopes of hazard curve. Table 5 shows the results of the theoretical collapse risk in these two sites. The nominal slope of the hazard curve ( $K_H$ ) in Guran is 2.57, while for Ahmadabad, the  $K_H$  is calculated to be 1.5. Such a difference has led to MCE values of 0.36 g and 0.59 g for Guran and Ahmadabad, respectively. According to the obtained results, despite the same DBE, the seismic risk in Ahmadabad is 1.74 times that of Guran. These results justify the high levels of the collapse risk in the SSZ.

The case of SSZ is a good example that explains why basing the seismic design on 475 years return period GM has led to the design of structures with lower reliability levels in the low-to moderate-hazard regions, which have severe earthquakes rarely. To treat the problem of these so-called “low-probability/high-consequence” earthquakes, many studies have proposed a transitioning to lower exceedance probabilities in national design provisions (Adams et al. 2000; Tsang 2011; Allen 2020). That is why modern codes in the US and Canada changed the reference hazard level from 10 to 2% in

50 years EP. The effect of this increase in the reference hazard level on the distribution of the theoretical collapse risk will be discussed in the next section.

Figure 10 shows the effects of the slopes of hazard curves on the risk-targeting results based on DBE. According to this Figure, it can be observed that the theoretical probability of collapse and the risk coefficients decrease with increasing the  $K_H$  values. In other words, the risk-targeting approach considers the slope of the hazard curve in determining the design GM in each site. As stated by Spillatura et al. (2019), from a computational point of view, the generic fragility curve is essentially a mechanism for weighting the effect of the hazard curve shape (or its local slope) and taking it into account when estimating the risk that is targeted by the procedure.

In this study, numerical integration has been used to calculate the risk integral [Eq. (1)]. However, there is also a closed-form solution for solving this integral, provided by Cornell (1994). Assuming a generic fragility function [similar to Eq. (3)], it can be proved that the risk of collapse is obtained from Eq. (5). Mathematical proof for this equation is provided in “Appendix” A.

$$\lambda_C = H(C_X) \cdot e^{0.5 \cdot K_H^2 \cdot \beta^2 + \Phi^{-1}(X) \cdot K_H \cdot \beta} \tag{5}$$

Using Eq. (5) allows us to examine the effect of the slope of the hazard curve on the risk of collapse in a more general way. By placing DBE as  $C_X$  in Eq. (5) and assuming different values of  $X$  and  $\beta$ , the risk of collapse is obtained for hazard curves with different slopes. Figure 11 shows the relation between the collapse risk and the parameter  $K_H$  for different combinations of  $X$  and  $\beta$ . As expected, in different cases, the risk of collapse decreases with increasing  $K_H$ . The rate of change in risk decreases with increasing  $\beta$ . An important justification for this is that Cornell’s approximate method for solving the risk integral is somewhat erroneous. Increasing the  $\beta$  and  $K_H$  increases the amount of this error. As stated by Cornell (1994), for very steep slopes and very broad capacity distributions (high values of  $K_H$  and  $\beta$ ), the amount of risk calculated by this method is overestimated.

Although the values of the probability of collapse are sensitive to the parameters  $X$  and  $\beta$ , the trends discussed in this section do not change with these parameters. Results in this section show that the computed probability of collapse is higher in low hazard areas. If the mid-range of collapse risk is selected as the target risk, that causes an increase in design GM in low hazard areas and, conversely, decreasing design GM in high hazard sites. The assumption of a fixed value of  $X$  causes an underestimation in the collapse capacity of

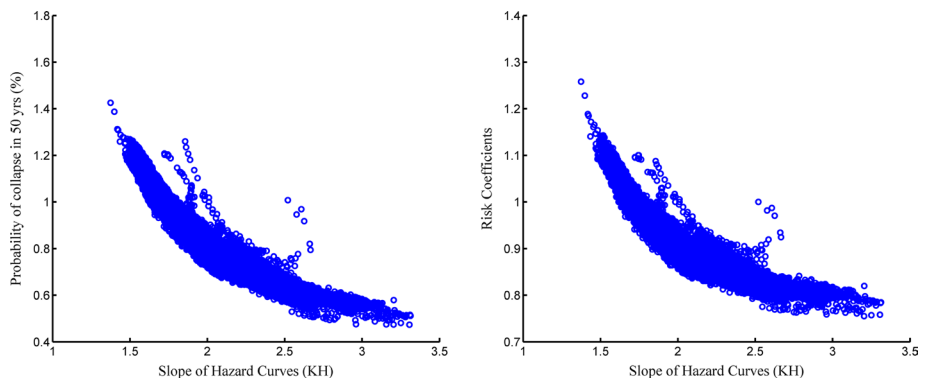


**Fig. 10** Relation of the slope of hazard curves ( $K_H$ ) and **a** theoretical collapse risk, **b** risk coefficients

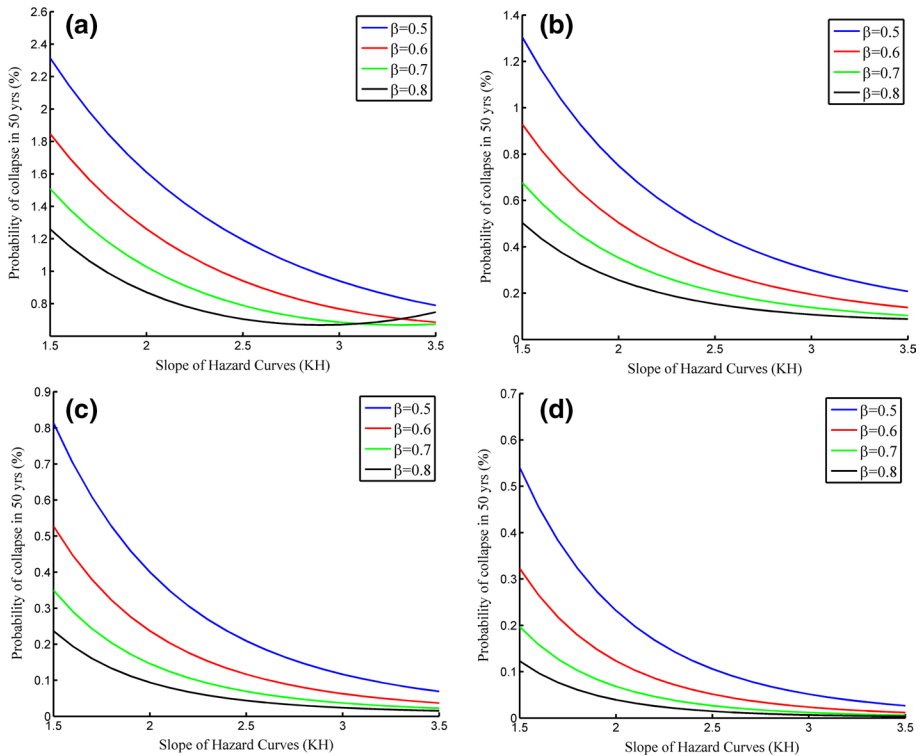


**Fig. 11** Relation of the slope of hazard curves ( $K_H$ ) and collapse risk assuming **a**  $X = 10^{-2}$ , **b**  $X = 10^{-3}$ , **c**  $X = 10^{-4}$ , **d**  $X = 10^{-5}$

buildings in low hazard sites. Moreover, as discussed earlier, the  $K_H$  values are generally lower in low hazard sites. We believe that combining these two facts has led to the opposing trend of the theoretical collapse risk and seismic hazard in the first case. It can be claimed that by taking the slope of hazard curves into account, the risk-targeting could harmonize the probability of collapse of buildings in sites with the same hazard in terms of DBE (like the case presented in Fig. 9). Nevertheless, this method could not have such an impact in areas of different hazard levels.

### 4.2 Risk-targeting based on MCE

In this case, the generic fragility function was generated based on the MCE values at each point of the country. The parameters  $X$  and  $\beta$  assumed to be  $10^{-1}$  and 0.80, respectively. Figure 12 shows the spatial distribution of the theoretical collapse probability for this case. Compared to the previous case, the trend of changes in seismic risk with the hazard is somehow different and seems more realistic. The CoV of the theoretical collapse risk is 11%, which is two times lower than the previous case. Generally, basing the seismic design on the MCE level leads to less variation in the probability of collapse in the country. A similar result for the US has been reported by Luco et al. (2007). Also, Heidebrecht (1999) and Adams et al. (2000) stated that the 2% in 50 years hazard results are considered a better

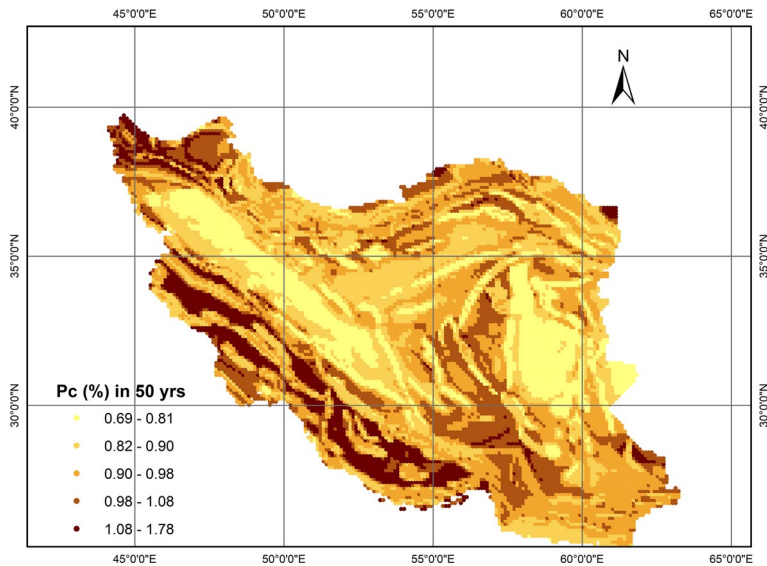
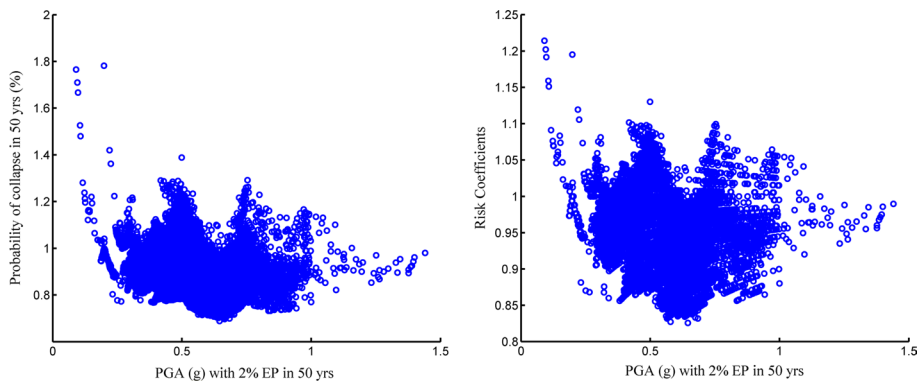


**Fig. 12** Spatial distribution of the theoretical risk of collapse (%) in Iran, considering 10% collapse probability given MCE shaking and  $\beta=0.8$

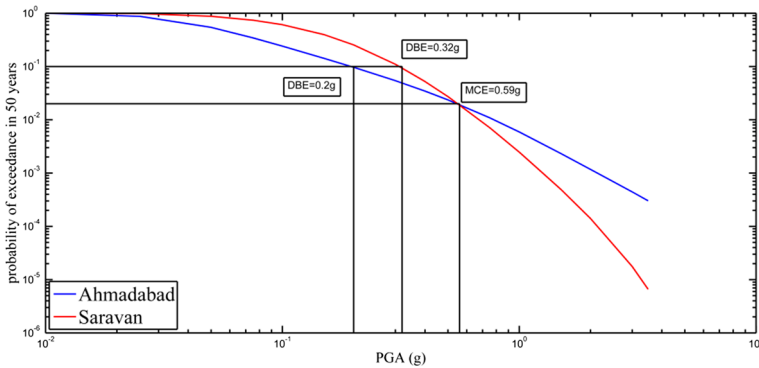
basis for achieving a uniform level of building safety across Canada, as they are closer to the acceptable frequency of collapse.

Figure 13 shows the trend of changes in the theoretical collapse probability with MCE changes. According to this Figure, there is not a specific trend between the risk-targeting results and the seismic hazard in this case. However, it can be claimed that the risk-targeting approach decreases the MCE values in most cases. The mean of calculated  $C_R$  values is 0.95, with a 0.05 standard deviation.

As can be observed in Fig. 10, the lowest probability of collapse is calculated for the SSZ. Establishing the MCE level has increased the design GM in this area up to three times. Consequently, the theoretical risk of collapse significantly decreased in the SSZ, which has led to a decrease in the MCE values in this area up to 15%. Figure 14



**Fig. 13** Relation of seismic hazard in terms of MCE and **a** notional collapse risk, **b** risk coefficients



**Fig. 14** Examples of PGA hazard curves for Ahmadabad and Saravan

shows an example of hazard curves for Ahmadabad (located in the SSZ) and Saravan (in Southeastern Iran) with different seismicity levels. The values of theoretical collapse risk for these sites are presented in Table 6. According to Table 6, for these two sites with the same MCE, the site with a higher  $K_H$  has a higher collapse risk. The reason for this is that, in Saravan, which has a higher  $K_H$ , the GMs less than the MCE have higher probabilities. For this particular case, these GMs have a relatively higher contribution to the collapse risk than the ones greater than the MCE.

The relationship between the  $K_H$  and the probability of collapse and  $C_R$  values is shown in Fig. 15. It can be observed that there is a direct relationship between the  $K_H$  and the theoretical probability of collapse, which is in contrast to the results of the previous section. A look back at Fig. 14 and Table 6 justifies the reason for this. For two sites with the same MCE, a higher  $K_H$  equals a higher DBE and, therefore, higher collapse risk.

Similar to the previous case, by placing MCE as  $C_X$  in Eq. (5) and assuming different values of  $X$  and  $\beta$ , the risk of collapse is obtained for hazard curves with different slopes. Figure 16 shows that the trend discussed above is mainly a result of the parameter  $X$  selected for this case. For instance, if  $X$  is selected equal to or less than  $10^{-2}$ , the trend will be reversed.

**Table 6** Comparison of the results of the theoretical collapse risk for Ahmadabad and Saravan

	DBE (g)	MCE (g)	MCE/DBE	$K_H$	Probability of collapse in 50 years (%)
Ahmadabad	0.20	0.59	2.90	1.5	0.73
Saravan	0.32	0.59	1.86	2.66	1.01

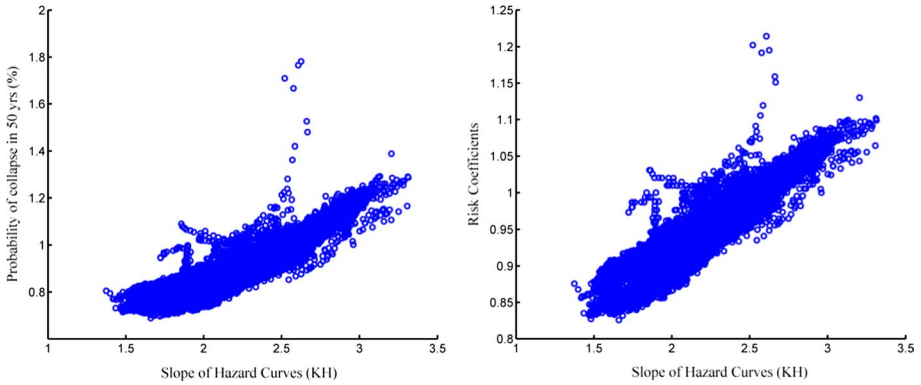


**Fig. 15** Relation of the slope of hazard curves ( $K_H$ ) and **a** theoretical collapse risk, **b** risk coefficients

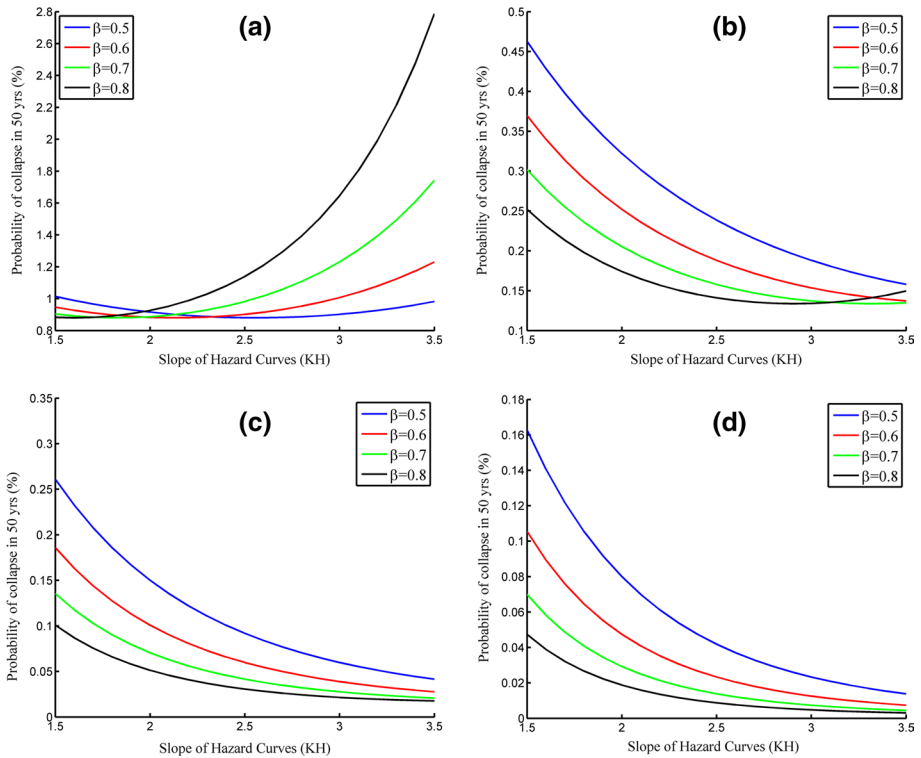


**Fig. 16** Relation of the slope of hazard curves ( $K_H$ ) and collapse risk assuming **a**  $X=10^{-1}$ , **b**  $X=10^{-2}$ , **c**  $X=10^{-3}$ , **d**  $X=10^{-4}$

### 5 Use of building-specific fragility function in the risk-targeting framework

As discussed earlier, the results of a study by Martins et al. (2018) Showed that for RC buildings designed to different levels of design PGA in Europe (ranging from 0.05 g to



0.40 g), the parameter X varies from  $10^{-5}$  to  $10^{-2}$ . Findings of the study of Martins et al. (2018) were later used to establish the relationships between the design PGA (dsgPGA) and the median ( $\theta$ ) and logarithmic standard deviation ( $\beta$ ) of the collapse fragility functions, which eventually led to the development of a building-specific fragility function for code-conforming RC buildings in Europe (Crowley et al. 2018). Equation (6) shows the fragility function developed by Crowley et al. (2018). This function was used by Crowley et al. (2018) to develop risk-targeted design maps for Greece.

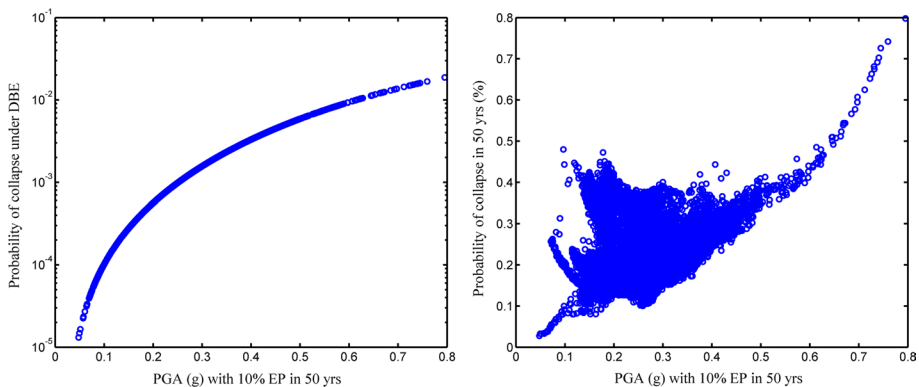
$$\begin{cases} \theta = 8.578 \times dsgPGA + 0.19 \\ \beta = 0.595 \times dsgPGA + 0.573 \end{cases} \quad (6)$$

To investigate the effects of the use of building-specific fragility function on the risk-targeting results, we used Eq. (6) to recalculate the distribution of the collapse risk in Iran. It should be noted that the fragility function was developed for RC buildings designed to EC8 and cannot be extended to Iranian code-conforming buildings. However, to examine the idea of developing a building-specific fragility function for Iranian buildings, this function has been used in this study.

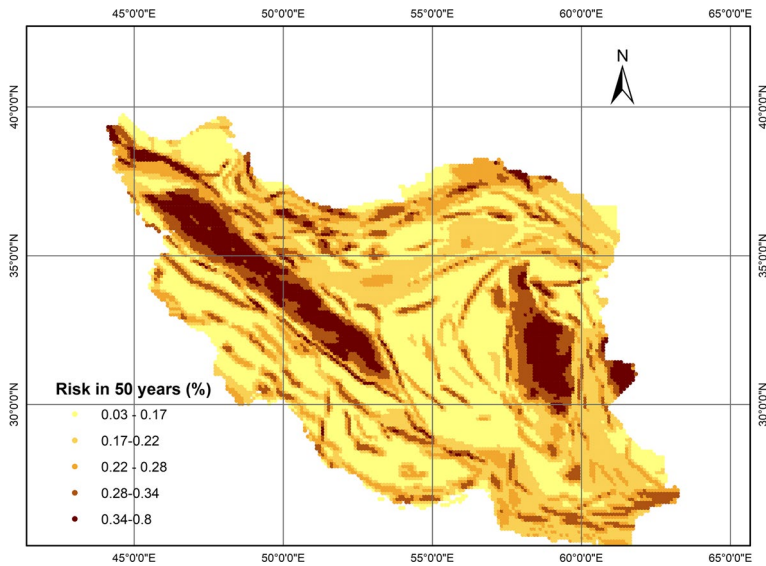
Figure 17a indicates that using Eq. (6), the parameter X increases with increasing design PGA. As shown in Fig. 17b, the probability of collapse of buildings increases proportionally with the increase in seismic hazard.

Figure 18 shows the spatial distribution of the risk of collapse in the country. As expected, the same trend of seismic hazard and seismic risk was observed in this case. The effect of the low slope of hazard curves in the central regions of the country is also evident in this case.

This section shows that the application of building-specific fragility functions could greatly improve the changes made by the risk-targeting approach. Similar results can be seen in the study of Gkimprixis et al. (2020), which used site-specific fragility functions to develop risk-targeted design maps for Europe. Nonetheless, it is relevant to note that the resulting risk-targeted design GMs, in this case, would be building-specific. In other words, fragility functions similar to the one in Eq. (5) should be developed for different building typologies designed according to a reference seismic code. Therefore, it should be noted that this method has a very high computational cost.



**Fig. 17** a Relation of the parameter X with EMME14 DBE, b Relation of the risk of collapse (%) in 50 years and EMME14 DBE based on the building-specific fragility function developed by Crowley et al. (2018)



**Fig. 18** Distribution of risk of collapse (%) in 50 years in Iran using building-specific fragility function developed by Crowley et al. (2018)

## 6 Discussions

In this study, the results of the risk-targeting approach for Iran were investigated in two cases: once considering 10% EP in 50 years GM (DBE), and then considering 2% EP in 50 years GM (MCE) as the reference seismic hazard level. The main conclusions of this study are as follows:

- Using the analysis of the mean PGA hazard curves from EMME14, the distribution of the slope of hazard curves ( $K_H$ ) in the country was presented. It was found that the  $K_H$  values vary considerably with locations in the country. The mean of MDR values is 2.11, with a dispersion of 0.29. The parameter  $K_H$  is generally lower in low- to moderate- hazard regions. The lowest  $K_H$  values were calculated for the SSZ. The MDR values in this area reach up to 3.00. According to EMME14 results, this area is exposed to “low-probability/high-consequence” earthquakes.
- In the first case, the risk-targeting was performed based on DBE values. From the results, it was found that there is an opposing trend between seismic hazard and the theoretical probability of collapse in the country. Therefore, the risk-targeting has increased DBE GMs in low hazard sites and decreased them in high hazard sites. The reasons for this trend are assuming a fixed  $X$  for all over the country and lower  $K_H$  in low- to moderate- hazard regions. In this case, the theoretical collapse risk for the SSZ reaches up to 1.13% in 50 years.
- In the second case, the risk-targeting was performed based on MCE values. It was found that basing the seismic design on the MCE level leads to a more uniform collapse risk across the country. No specific trend was observed between hazard and collapse risk. The theoretical collapse risk has a direct relation with the parameter

$K_H$ . Establishing the MCE level has reduced the theoretical probability of collapse in the SSZ to 0.73% in 50 years.

According to the results of the RINTC project (Iervolino et al. 2018), the seismic design of buildings for UHGM leads to significantly higher levels of seismic risk in areas of high hazard. Therefore, to achieve a more uniform distribution of seismic risk, we should increase the UHGM in high hazard regions or decrease them in low hazard regions. The results of this study showed that employing a generic fragility function, the risk-targeting approach does not cause such modifications. The risk-targeting could only harmonize the probability of collapse of buildings in sites with the same UHGM. Nevertheless, this method could not have such an impact on areas of different hazard levels.

In the case of the US, this is somewhat different. Given the higher seismic hazard in the Western US, the probability of collapse of buildings in these areas is considerably higher compared to Central and Eastern US. The risk-targeting approach has been applied only in the probabilistic portion of the US and has led to a reduction in the MCE values in the Central and Eastern US. Therefore, it can merely be claimed that this approach has led to harmonize the seismic risk in the US. Moreover, implementing this approach for the MCE level would have more rational results.

The strength of the risk-targeted approach is that it considers the hazard curve slope to determine the design GM. In other words, this method distinguishes between two sites with the same UHGM but different  $K_H$ . In contrast, the disadvantage of this method is how to define the generic fragility function. As shown in this paper, the (unrealistic) assumption of a fixed probability of collapse under the design GM ( $X$ ) for buildings in different hazard levels causes an overestimated calculation of the theoretical collapse risk in low hazard regions. Moreover, as stated by Spillatura et al. (2019), the generic fragility function used in risk-targeting is not building-specific. To solve these issues, recent studies such as Crowley et al. (2018) and Gkimprxis et al. (2020) have implemented the risk-targeting approach using analytical fragility functions which were developed for the RC moment-resisting frame buildings designed to different levels of seismicity in Europe. Application of building-specific fragility functions in risk-targeting has much better results but at a much higher computational cost.

**Acknowledgment** The first author would like to thank Athanasios Gkimprxis for the valuable discussions on the subject of risk-targeting. This paper has greatly benefited from the helpful comments of the Associate Editor Professor Carlos Sousa Oliveira, and an anonymous reviewer. Also, discussions with Professor Mehdi Zare and Professor Manuel Berberian on the Sanandaj-Sirjan zone are gratefully acknowledged.

**Funding** The research described in this paper was supported by the Iran National Science Foundation under the Grant No. 99007088.

## Appendix A: Mathematical proof for Eq. (5)

The basic premise of the closed-form solution for the risk integral developed by Cornell (1994) is to fit the hazard curve to a power function such as Eq. (7).

$$H(IM) = K_0 \cdot IM^{-K_H} \quad (7)$$

where  $K_0$  is an appropriate constant, and  $K_H$  is the logarithmic slope of the hazard curve defined by Eq. (4). Assuming a log-normal fragility function with a median collapse

capacity,  $C_{50\%}$ , and a logarithmic standard deviation,  $\beta$ , the annual collapse risk is obtained using Eq. (8).

$$\lambda_C = H(C_{50\%}) \cdot e^{0.5 \cdot K_H^2 \cdot \beta^2} \quad (8)$$

The relation between the 50th-percentile and another percentile (X-percentile) of the collapse capacity is as Equation (9).

$$C_X = C_{50\%} \cdot e^{\Phi^{-1}(X) \cdot \beta} \quad (9)$$

Substituting Eq. (9) into Eq. (8) gives Eq. (5) in the paper.

$$\lambda_C = H(C_X) \cdot e^{0.5 \cdot K_H^2 \cdot \beta^2 + \Phi^{-1}(X) \cdot K_H \cdot \beta} \quad (10)$$

## References

- Adams J, Halchuk S, Weichert DH (2000) Lower probability hazard, better performance? Understanding the shape of the hazard curves from Canada's fourth generation seismic hazard results. Proceedings of the 12th World Conference on Earthquake Engineering, Auckland, New Zealand. Paper 1555 on CD-ROM. Auckland: 2000
- ASCE (2002) Minimum design loads for buildings and other structures (ASCE 7–02). American Society of Civil Engineers, Reston, VA
- ASCE (2010) Minimum design loads and associated criteria for buildings and other structures, ASCE/SEI7–10. American Society of Civil Engineers, Reston
- Atkinson GM, Boore DM (2006) Earthquake ground-motion prediction equations for eastern North America. *Bull Seismol Soc Am* 96(6):2181–2205
- Allen TI (2020) Seismic hazard estimation in stable continental regions. *Bull N Z Soc Earthq Eng* 53(1):22–36. <https://doi.org/10.5459/bnzsee.53.1.22-36>
- Ambraseys NN, Melville CP (1982) A history of persian earthquakes. Cambridge University Press, New York, p 219
- Atkinson GM (2004). An overview of developments in seismic hazard analysis. In: Proceedings of thirteenth world conference on earthquake engineering. Paper no. 5001
- Cornell CA (1994) Risk based structural design. Paper presented at the Symposium on Risk Analysis, Ann Arbor (MI)
- Cito P, Iervolino I (2020) Peak-over-threshold: Quantifying ground motion beyond design. *Earthq Eng Struct Dyn* 49:458–478. <https://doi.org/10.1002/eqe.3248>
- Campbell KW (2003) Prediction of strong ground motion using the hybrid empirical method and its use in the development of ground–motion (attenuation) relations in eastern North America. *Bull Seismol Soc Am* 93(3):1012–1033
- Crowley H, Silva V, Martins L (2018). Seismic design code calibration based on individual and societal risk. In: Proceedings of the 16th european conference on earthquake engineering. June, 2018. p 18–21. [Thessaloniki, Greece]
- Cornell CA (1968) Engineering seismic risk analysis. *Bull Seismol Soc Am*. 58(5):1583–1606. [https://doi.org/10.1016/0167-6105\(83\)90143-5](https://doi.org/10.1016/0167-6105(83)90143-5)
- Danciu L et al. (2017) The 2014 earthquake model of the Middle East: seismogenic sources. *Bull Earthq Eng* pp 1–32
- Douglas J, Ulrich T, Negulescu C (2013) Risk-targeted seismic design maps for mainland France. *Nat Hazards* 65(3):1999–2013. <https://doi.org/10.1007/s11069-012-0460-6>
- FEMA (2000) NEHRP recommended provisions for seismic regulations for new buildings and other structures, FEMA 369. Federal Emergency Management Agency, Washington, DC
- FEMA (2009) Quantification of Building Seismic Performance Factors, FEMA P-695, prepared by the applied technology council for the federal emergency management agency, Washington, D.C
- Frankel A (2003) [Comment on “should memphis build for California's earthquakes?”] from AD Frankel. *Eos Trans Am Geophys Un*. <https://doi.org/10.1029/2003EO290005>

- Frankel A (2004) How can seismic hazard around the New Madrid seismic zone be similar to that in California? *Seismol Res Lett* 75:575–586
- Gkimprxis A, Douglas J, Tubaldi E, Zonta D (2018) Development of fragility curves for use in seismic risk targeting
- Gkimprxis A, Tubaldi E, Douglas J (2019) Comparison of methods to develop risk-targeted seismic design maps. *Bull Earthq Eng* 17:3727–3752. <https://doi.org/10.1007/s10518-019-00629-w>
- Gkimprxis A, Tubaldi E, Douglas J (2020) Evaluating alternative approaches for the seismic design of structures. *Bull Earthquake Eng* 18:4331–4361. <https://doi.org/10.1007/s10518-020-00858-4>
- Heidebrecht AC (1999) Implications of new Canadian uniform hazard spectra for seismic design and the seismic level of protection of building structures. In: *Proceedings 8th Canadian conference on earthquake engineering*, Vancouver 13–16th June 1999, p 213–218
- ICBO (1997) Uniform building code, structural engineering provisions, Vol 2, 1997 edition, pp 2-161 to 2-163. In: *International conference of building officials*, Whittier, California
- Iervolino I, Spillatura A, Bazzurro P (2018) Seismic reliability of code conforming Italian buildings. *J Earthq Eng* 22:5–27. <https://doi.org/10.1080/13632469.2018.1540372>
- Jalayer F, Cornell CA (2003) A technical framework for probability-based demand and capacity factor design (DCFD) seismic formats. PEER Report 2003/08, Pacific Earthquake Engineering Center, College of Engineering, University of California Berkeley, November
- Luco N, Ellingwood BR, Hamburger RO, Hooper JD, Kimball JK, Kircher CA (2007) Risk-targeted versus current seismic design maps for the conterminous United States. In: *SEAOC 2007 convention proceedings*
- Martins L, Silva V, Bazzurro P, Marques M (2018) Advances in the derivation of fragility functions for the development of risk-targeted hazard maps. *Eng Struct* 173:669–680. <https://doi.org/10.1016/j.engstruct.2018.07.028>
- Nadimi A, Konon A (2012) Strike-slip faulting in the central part of the Sanandaj-Sirjan Zone, Zagros Orogen. *Iran J Struct Geol* 40:2–16. <https://doi.org/10.1016/j.jsg.2012.04.007>
- Safaei H (2009) The continuation of the Kazerun fault system across the Sanandaj-Sirjan zone (Iran). *J Asian Earth Sci* 35:391–400. <https://doi.org/10.1016/j.jseaes.2009.01.007>
- Silva V, Crowley H, Bazzurro P (2016) Exploring risk-targeted hazard maps for Europe. *Earthq Spectra* 32(2):1165–1186
- Spillatura A, Vamvatsikos D, Bazzurro P, Kohrangi M. (2019) Issues in Harmonization of Seismic Performance via Risk Targeted Spectra. In: *13th international conference on applications of statistics and probability in civil engineering*, ICASP13, Seoul, South Korea
- Stein S, Tomasello J, Newman A (2003) Should Memphis build for California's earthquakes? *Eos Trans Am Geophys Un*. <https://doi.org/10.1029/2003EO190002>
- Taherian AR, Kalantari A (2019) Risk-targeted seismic design maps for Iran. *J Seismol* 23:1299. <https://doi.org/10.1007/s10950-019-09867-6>
- Toro GR, Abrahamson NA, Schneider JF (1997) Model of strong ground motions from earthquake in central and eastern North America: best estimates and uncertainties. *Seismol Res Lett* 68(1):41–57
- Tsang H (2011) Should we design buildings for lower-probability earthquake motion? *Nat Hazards* 58:853–857. <https://doi.org/10.1007/s11069-011-9802-z>
- Ulrich T, Negulescu C, Douglas J (2014) Fragility curves for risk-targeted seismic design maps. *Bull Earthq Eng* 12(4):1479–1491. <https://doi.org/10.1007/s10518-013-9572-y>

**Publisher's Note** Springer Nature remains neutral with regard to jurisdictional claims in published maps and institutional affiliations.